0026-895X/95/010089-09$3.00/0

MOLECULAR PHARMACOLOGY, 48:89–97 (1995).

Voltage- and Frequency-Dependent Pentobarbital Suppression of Brain and Muscle Sodium Channels Expressed in a Mammalian Cell Line

BENNO REHBERG, ERIC BENNETT, YONG-HONG XIAO, SIMON R. LEVINSON, and DANIEL S. DUCH

Departments of Anesthesiology and Physiology, Cornell University Medical College, New York, New York 10021 (B.R., Y.-H.X., D.S.D.), and Department of Physiology, University of Colorado Health Sciences Center, Denver, Colorado 80262 (E.B., S.R.L.)

Received November 4, 1994; Accepted April 3, 1995

SUMMARY

The voltage- and frequency-dependent interactions of pentobarbital with voltage-gated sodium channels were examined in whole-cell patch-clamp recordings. Using rat brain IIA and rat muscle rSkM1 sodium channels expressed in stably transfected Chinese hamster ovary cell lines, it was found that pentobarbital reduced peak inward sodium currents with IC_{50} values of 1.2 mM (brain) and 1.0 mM (muscle). Analysis of steady state channel availability curves revealed two distinct effects of pentobarbital on both channel isoforms, i.e., a voltage-independent current reduction and an additional hyperpolarizing shift in the voltage dependence of channel availability. The latter effect leads to a voltage dependence of pentobarbital potency. Pentobarbital was also found to slow channel recovery after depolarization, yielding an additional use-dependent component of current suppression. Use-dependent block was enhanced by higher stimulation frequencies, longer pulse durations, and more depolarized holding and pulse potentials. All effects were identical for both channels. These findings can be explained in terms of the modulated receptor hypothesis and are consistent with a preferential interaction of pentobarbital with the inactivated channel state. As a consequence, actual pentobarbital potency would depend largely on experimental conditions or, *in vivo*, on the physiological parameters of a particular cell.

Voltage-dependent sodium channels mediate the propagation of action potentials along nerve and muscle membranes by undergoing a series of conformational transitions in response to changes in membrane potential. At rest, the membrane potential is hyperpolarized and sodium channels are in a "closed" state. During an action potential, the membrane is depolarized and the channel transiently opens or activates, allowing sodium to cross the membrane into the cell. The channel then inactivates, preventing further sodium flux. These conformational states are related to the opening and closing of separate activation and inactivation gates.

Due to their central role in signal transmission, sodium channels are the targets of a large number of diverse pharmacological agents, including local anesthetics, anticonvulsants, and antiarrhythmic agents (1–3). The modulated receptor hypothesis (4, 5) proposes that many of these drugs have different affinities for the various conformational states of the channel, as reflected in their measured pharmacological behavior (1). Adding to the complexity of these interactions, it has recently been found that wide diversity exists in sodium channel structure among channels from different tissues, as well as within the CNS (6, 7). It is not known how these structural differences affect the pharmacological responses of the channel.

General anesthetics are another group of pharmacological agents that alter sodium channel function. Due to experimental difficulties, most previous studies examined anesthetic effects on sodium channels from tissues other than the CNS (8–11). Recent experiments using sodium channels from human brain incorporated into planar lipid bilayers in the presence of the alkaloid activator batrachotoxin have indicated that general anesthetics alter the function of CNS channels at clinically relevant concentrations (12, 13). These single-channel studies have shown that a representative barbiturate anesthetic, pentobarbital, has both similar and dissimilar effects on brain and muscle-derived sodium channels (14). However, bilayer studies used homogenized tissues and therefore did not allow the determination of anesthetic interactions with specific channel isoforms of known structure. Furthermore, channels in bilayers are modified by toxins, and the results need to be further examined with non-toxin-modified channel preparations.

To further investigate the effects of channel structural

This work was supported by National Institutes of Health Grants NS15879 (S.R.L.) and GM41102 (D.S.D.).

ABBREVIATIONS: CNS, central nervous system; CHO, Chinese hamster ovary; HEPES, 4-(2-hydroxyethyl)-1-piperazineethanesulfonic acid; V_h, potential for half-maximal effect.

diversity on general anesthetic interactions, as well as the molecular mechanisms by which pentobarbital modifies sodium channels, we have examined pentobarbital modification of specific sodium channel isoforms (the rat brain type IIa and the rat muscle rSkM1 sodium channels) expressed in stably transfected CHO cells. The rat brain IIA/CHO cell system was previously used to examine the interactions of several other drug classes with these channels (3), and the results were explained in the context of the modulated receptor hypothesis (4). We therefore focused our present study to test whether the predictions of this hypothesis also hold true for pentobarbital inhibition of sodium channels from both brain and muscle.

Materials and Methods

Cell culture. Two stably transfected CHO cell lines were used; the CNaIIA-1 cell line (a gift from Dr. William Catterall, University of Washington, Seattle, WA) expresses the rat brain IIA sodium channel (15, 16), and the other cell line (CrSkM-1) was transfected with the mammalian expression vector pZEM228 (a gift from Dr. Eileen Mulvihill, Zymogenetics, Seattle, WA) containing cDNA encoding the rat muscle rSkM1 sodium channel (17, 18). Both vectors contain the *neo* selection gene, conferring resistance to the aminoglycoside antibiotic G418.

Both cell lines were grown in RPMI 1640 medium (GIBCO) containing 10% fetal bovine serum and 1% penicillin/streptomycin mixture (GIBCO), as well as 200 μg/ml G418 to select for transfected cells. All cells were cultured in 25-cm^2 polystyrene culture flasks (Corning) at 37° in humidified room air containing 5% CO_2. For electrophysiological recordings, cells were transferred to 60-mm Petri dishes (Becton Dickinson).

Electrophysiology. Cells were used 2–3 days after transfer, before the cell layer became confluent. For electrophysiological measurements, the culture medium was replaced by an extracellular solution containing 130 mM NaCl, 4 mM KCl, 1.5 mM $CaCl_2$, 1.5 mM $MgCl_2$, 5 mM glucose, and 5 mM HEPES, adjusted to pH 7.4 with NaOH. All solutions were filtered through 0.22-μm filters (Millipore, Bedford, MA). Recordings were made at room temperature (23.5 ± 1.0°).

Sodium currents were studied using the whole-cell configuration of the patch-clamp recording technique (19), using a standard patch-clamp amplifier (Axopatch 200; Axon Instruments) controlled by commercially available software (pCLAMP; Axon Instruments) on a standard PC. Currents were filtered at 5 kHz, digitized, and recorded to hard disk. Capacitative transients and series resistance were measured and compensated using the internal compensation circuitry of the amplifier; active series resistance compensation was used to compensate 70–85% of the series resistance. Average series resistance before compensation was 3.9 MΩ for cells expressing brain IIa sodium channels and 3.6 MΩ for those expressing muscle sodium channels, and the average cell capacitances were 16.4 pF and 16.8 pF, respectively. Patch-clamp pipettes were pulled from micropipette glass (Drummond, Broomall, PA) and filled with an intracellular solution containing 10 mM NaCl, 90 mM CsF, 60 mM CsCl, and 6 mM HEPES, adjusted to pH 7.4 with NaOH. Cells with currents larger than 5 nA (because of increasing series resistance error) or smaller than 0.5 nA (because of interference with possible small endogenous sodium currents in CHO cells) were excluded; the average current of the 21 cells expressing the rat brain IIa sodium channel included in this study was 2.2 ± 1.4 nA, and the 16 cells expressing rat muscle sodium channels had average currents of 3.6 ± 1.6 nA.

Pentobarbital (racemic mixture; Sigma Chemical Co., St. Louis, MO) was dissolved directly in the extracellular solution and applied via a superfusion pipette (flow rate, 0.5–0.8 ml/min) positioned close to the cell. Solutions with pentobarbital concentrations greater than 3.4 mM were prepared at alkaline pH (with NaOH), and the pH was then readjusted to 7.4. This increased the Cl^- concentration by 6 mM and the Na^+ concentration from 132 to 139.4 mM. Most experiments included the consecutive application of several drug concentrations and washout with pentobarbital-free extracellular solution.

Statistics. Curve fits were computed using a least-squares algorithm of commercially available software (SigmaPlot from Jandel Scientific and pCLAMP from Axon Instruments). Data are given as mean ± standard error, unless noted otherwise.

Results

Suppression of sodium currents by pentobarbital. Pentobarbital suppresses sodium currents elicited by stepping the potential from a resting value of −100 mV (held for 1.5 sec before each depolarization) to test potentials ranging from −60 to +100 mV (Fig. 1A). This effect occurs within seconds and can be reversed by washout with pentobarbital-free extracellular solution (Fig. 1B). Currents reverse around the Na^+ equilibrium potential (+63 mV) and can be blocked by tetrodotoxin (Fig. 1, B and C).

Peak currents were plotted versus test potential (Fig. 1C), and the minima of these curves (maximum inward sodium current) were used to calculate an estimate of current suppression (Fig. 2); IC_{50} values are 1.2 ± 0.2 mM (mean ± standard error of the fit) for brain IIa channels and 1.0 ± 0.1 mM for muscle channels. Suppression of brain IIa and muscle sodium currents is not significantly different (unpaired *t* test; *p* values are 0.25, 0.95, 0.97, 0.73, 0.69, and 0.15 for 0.42, 0.85, 1.7, 3.4, 5.1, and 6.8 mM pentobarbital, respectively).

Effect of pentobarbital on sodium channel steady state availability. Steady state inactivation or "h_∞" curves describe the voltage dependence of channel inactivation. However, when a channel modifier exhibits state-dependent drug binding, the number of channels available for opening may not be determined solely by inactivation but may also be altered by drug binding. For this reason, we use the term "steady state availability" to describe the data obtained with pentobarbital-modified channels.

Steady state availability was assessed by a two-pulse protocol comprising a 500-msec prepulse to potentials ranging from −150 to −20 mV followed by a 25-msec test pulse to −10 mV. The prepulse duration was sufficient to allow channel availability to reach a steady state at all prepulse potentials and drug concentrations (data not shown). Steady state availability plots were constructed by dividing the current measured after a given test pulse by the maximum current recorded (shown in Fig. 3 for controls and selected concentrations). The plots can be normalized either to the maximum current achieved with each pentobarbital concentration (Fig. 3A), representing h_∞ plots as described by Hodgkin and Huxley, or to the maximum current achieved before addition of pentobarbital (Fig. 3B), showing the reduction of current at each potential.

These data were fit to two-level Boltzman distributions, yielding V_h (the potential for half-maximal inactivation for control channels or half-maximal sodium channel availability in the presence of pentobarbital), *z* (the slope parameter of the curve), and I_{max} (the maximum sodium current at hyperpolarized potentials). The slope parameter, with one exception (3.4 mM) for the brain channel, is not significantly different from control at any pentobarbital concentration for either brain IIa or rat muscle channels (Table 1) (*p* values for

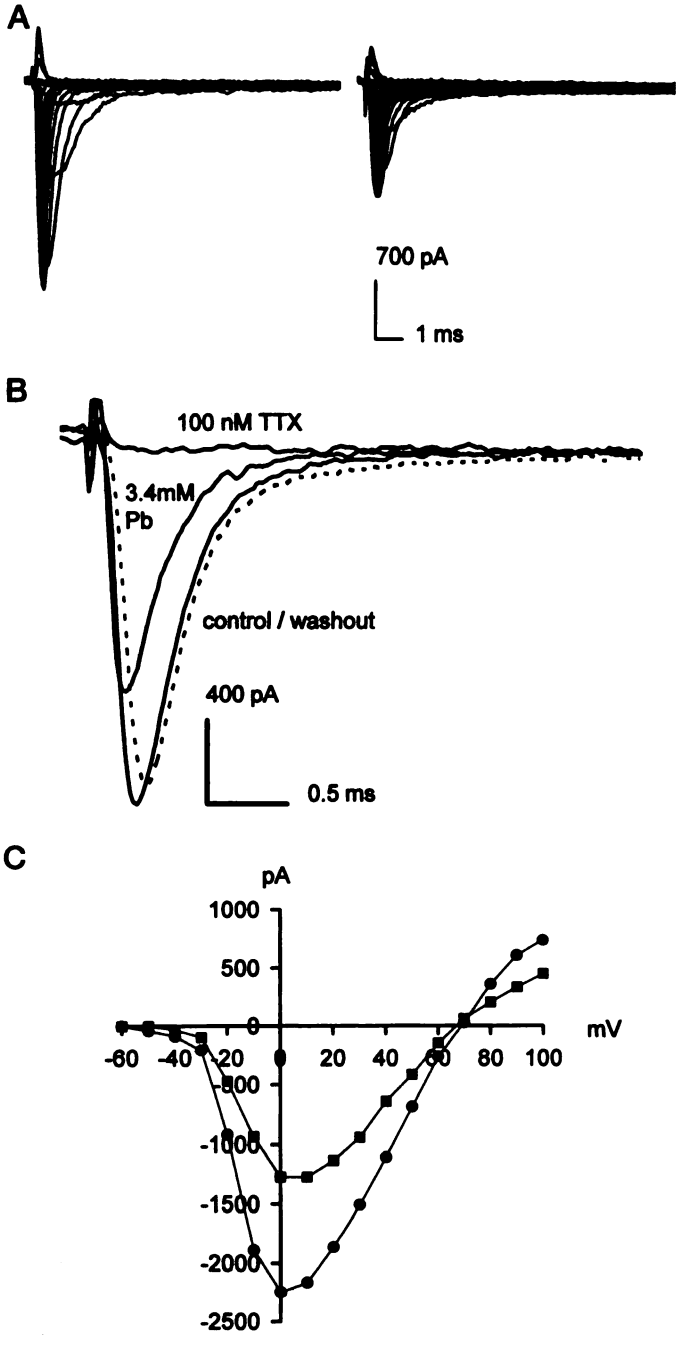

Fig. 1. Effect of pentobarbital on whole-cell sodium currents. A, Currents elicited by stepping the potential from −100 mV to test potentials varying from −60 to +100 mV (filter frequency, 5 kHz). Traces were obtained before (*left*) and after (*right*) superfusion with 3.4 mM pentobarbital, from a cell (cell capacitance, 15 pF; series resistance, 3.5 MΩ) expressing the rSkM1 muscle sodium channel. *Calibration bars*, 700 pA and 1 msec. B, Current traces elicited by a voltage step to +10 mV before, during, and after (*dashed line*) superfusion with 1.7 mM pentobarbital (*Pb*), as well as after superfusion with 100 nM tetrodotoxin (*TTX*), in a cell expressing the rSkM1 sodium channel. *Calibration bars*, 400 pA and 0.5 msec. C, Peak current-voltage relationship for the same cell as in A (●, control; ■, after superfusion with 3.4 mM pentobarbital).

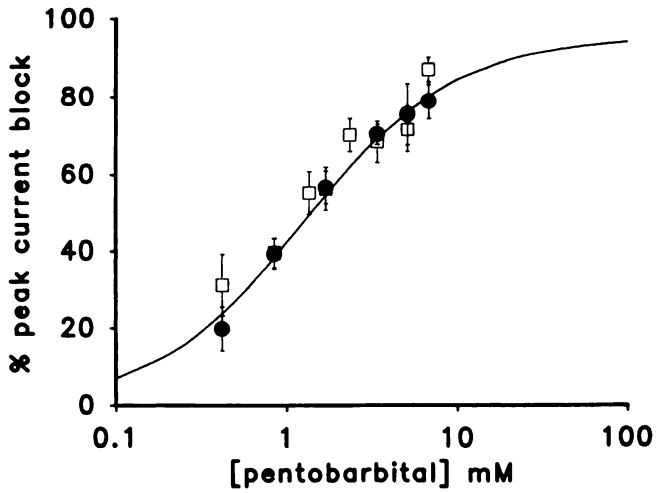

Fig. 2. Concentration-dependent reduction by pentobarbital of the maximum inward sodium current. Maximum inward sodium currents were obtained from peak sodium current versus voltage plots, such as shown in Fig. 1C. Data are averages (*error bars*, standard errors) from 31 cells expressing the brain sodium channel (●) and from 20 cells expressing the rSkM1 channel (□). Least-squares fit of the function $I = (I_{max} \cdot c)/(IC_{50} + c)$ to the data (*solid line*, brain) yields IC_{50} for pentobarbital of 1.2 ± 0.2 mM (mean ± standard error of the fit). A similar fit for the muscle channel yielded 1.0 ± 0.1 mM. Maximum suppression determined by the fit is 94% for brain channels and 92% for muscle channels. Differences in suppression of the peak sodium current are not significant between channel types (unpaired *t* test at all identical concentrations).

paired *t* tests are 0.60, 0.12, 0.62, 0.70, 0.53, and 0.11 for 0.42, 0.85, 1.7, 3.4, 5.1, and 6.8 mM pentobarbital for the muscle channel; for the brain channel the corresponding *p* values are 0.42, 0.29, 0.40, 0.03, 0.98, and 0.05).

V_h shows a reversible, concentration-dependent, hyperpolarizing shift after pentobarbital application for both types of sodium channels (Fig. 4A; Table 1). A time-dependent, hyperpolarizing shift of V_h in the absence of drugs has been reported for other whole-cell preparations (20, 21). Control experiments without pentobarbital application indicate no shift of steady state inactivation for up to 30 min (data not shown). In addition, the data obtained after washout of pentobarbital indicate that V_h returns close to control values (Table 1) even during the limited time span of washout in most experiments (3–6 min).

Dose-response curves for the pentobarbital-induced shift in V_h are shown in Fig. 4A. Values for this shift are statistically indistinguishable for rat brain and muscle channels at each pentobarbital concentration (unpaired *t* test; *p* values are 0.12, 0.28, 0.81, 0.10, 0.84, and 0.31 for 0.42, 0.85, 1.7, 3.4, 5.1, and 6.8 mM pentobarbital, respectively).

Pentobarbital suppression of the maximum sodium current at hyperpolarized prepulse potentials yields EC_{50} values of 1.26 ± 0.07 mM and 1.13 ± 0.10 mM for brain IIa and muscle channels, respectively (Fig. 4B). These EC_{50} values are similar to those obtained by measuring the reduction of peak inward current (Fig. 2). Differences in the reduction of the maximum current for brain IIa and muscle channels are not significantly different at any pentobarbital concentration (unpaired *t* test; *p* values are 0.75, 0.35, 0.76, 0.78, 0.48, and 0.50 for 0.42, 0.85, 1.7, 3.4, 5.1, and 6.8 mM pentobarbital, respectively). Due to the lack of data at higher concentrations (where the current is almost completely blocked), there is a high degree of uncertainty in the EC_{50} values for the V_h shift, but the EC_{50} values for this effect are higher than those for suppression at hyperpolarized prepulse potentials.

Voltage dependence of pentobarbital inhibition. The hyperpolarizing shift in sodium channel availability indi-

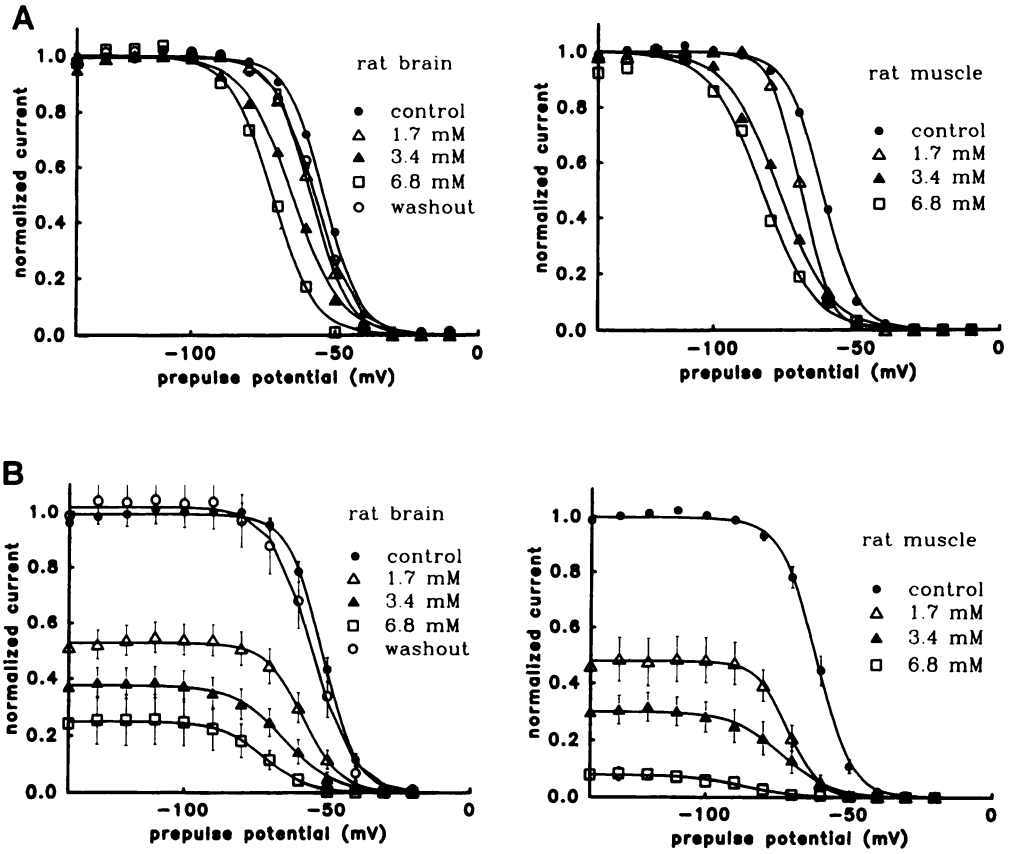

Fig. 3. Effect of pentobarbital on sodium channel inactivation. Sodium currents, elicited by test pulses to −10 mV after 500-msec prepulses to potentials varying from −150 to −10 mV, are plotted as a function of prepulse potential. Data are averages from 21 cells expressing brain sodium channels and eight cells expressing muscle sodium channels. A, Currents normalized to the maximum sodium current under each condition, comparable to h_∞ curves in classic Hodgkin-Huxley analysis (error bars were omitted; see B for errors of same data). B, Currents normalized to the maximum sodium current under control conditions, obtained from fits to two-level Boltzmann distributions.

TABLE 1

Effect of pentobarbital on sodium channel steady state availability

Potentials for half-maximal channel availability (V_h), slope parameters (z), and normalized maximum currents at hyperpolarized potentials (I_{max}) [I_{max}(control) = 1], yielded by fits of two-level Boltzmann distributions to channel availability data such as those shown in Fig. 3B, are given. Data are averages of the fit parameters for individual experiments (n, number of experiments); only averages ± standard errors of data points from at least three experiments are included.

Pentobarbital	Rat brain				Rat muscle			
	n	V_h	z	I_{max}	n	V_h	z	I_{max}
nM		mV				mV		
Control	32	−53.2 ± 1.2	5.2 ± 0.2	1	22	−63.0 ± 1.7	5.0 ± 0.3	1
0.42	13	−54.8 ± 1.0	7.2 ± 2.3	0.73 ± 0.08	8	−65.1 ± 2.3	6.8 ± 0.5	0.70 ± 0.06
0.85	21	−57.2 ± 1.5	6.3 ± 0.9	0.62 ± 0.05	8	−66.2 ± 2.4	6.9 ± 0.6	0.54 ± 0.04
1.36					8	−69.0 ± 2.9	6.4 ± 1.2	0.45 ± 0.06
1.70	21	−61.2 ± 2.0	6.9 ± 1.8	0.50 ± 0.05	8	−70.0 ± 2.6	6.5 ± 0.7	0.47 ± 0.08
2.38					10	−79.7 ± 3.6	5.0 ± 0.7	0.26 ± 0.06
3.40	22	−69.2 ± 2.7	4.3 ± 0.4	0.34 ± 0.04	12	−78.5 ± 3.5	4.6 ± 0.4	0.32 ± 0.05
5.10	5	−76.7 ± 11.7	5.3 ± 1.6	0.14 ± 0.08	8	−73.8 ± 4.3	7.1 ± 1.9	0.21 ± 0.05
6.80	7	−73.2 ± 5.0	4.2 ± 0.6	0.17 ± 0.03	7	−84.7 ± 5.8	8.1 ± 2.3	0.08 ± 0.02
Washout	18	−57.5 ± 2.0	4.8 ± 0.3	1.01 ± 0.13	4	−69.2 ± 4.0	5.3 ± 0.5	0.90 ± 0.16

cates a voltage dependence of pentobarbital inhibition. Pentobarbital reduces current more at depolarized prepulse potentials than at hyperpolarized potentials (Fig. 5). For currents elicited by voltage steps from prepulse potentials of −100 mV to a test potential of −10 mV, the IC_{50} of pentobarbital for brain IIa channels is 1.4 mM; for currents elicited by voltage steps from −60 mV to −10 mV, the IC_{50} is reduced by about one half, to 0.6 mM (Fig. 5A). This voltage dependence of pentobarbital inhibition occurs in the voltage range of sodium channel inactivation, as can be seen by plotting the IC_{50} values versus membrane potential (Fig. 5B). Muscle and brain IIa sodium channels have different voltage dependencies of inactivation (brain IIa sodium channels have an inactivation midpoint potential about 10 mV positive to that of muscle channels; see Fig. 3A and Table 1) but similarly shifted voltage dependencies of pentobarbital inhibition.

Effect of pentobarbital on the kinetics of channel availability. The hyperpolarizing shift in steady state channel availability may be due to an increase in the rate constant of conversion to nonavailable states (i.e., the rate constant of inactivation for control channels) and/or a decrease in the rate constant of recovery from nonavailable (inactive) states. At hyperpolarized potentials, we examined the time constant of channel recovery, using a three-pulse protocol including a first depolarizing, 10-msec, reference pulse to −10 mV, a recovery interval of variable duration (2.5–30 msec) at −100, −120, or −80 mV, and a second test pulse to −10 mV (Fig. 6). At all three potentials, the time constant for recovery is

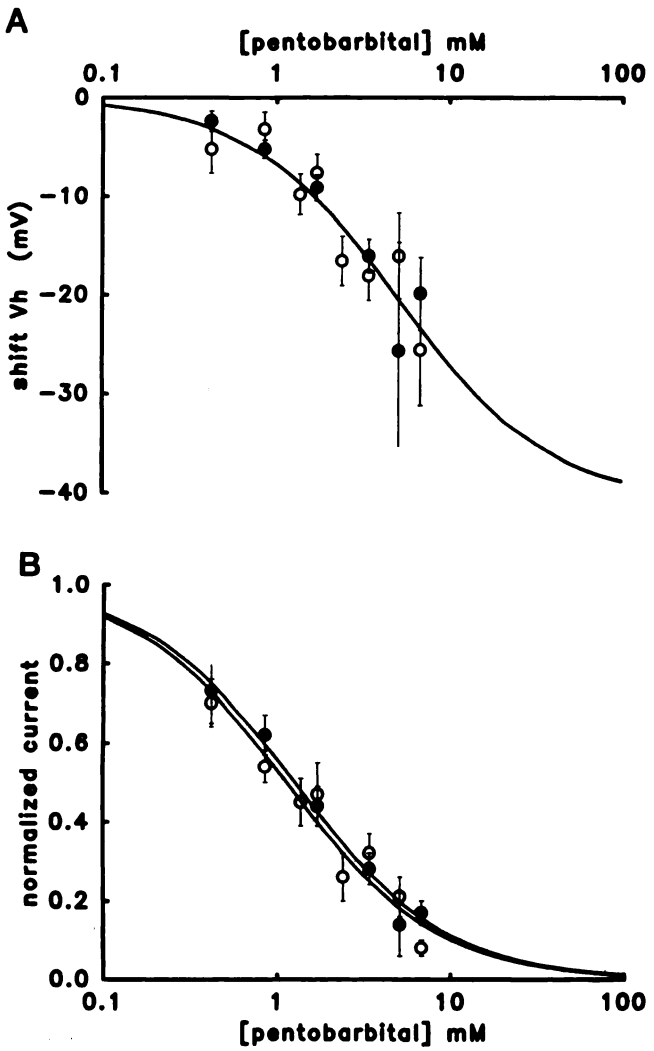

Fig. 4. Dependence of the parameters of steady state availability curves (●, brain channels; ○, muscle channels) on pentobarbital concentration. Data shown are averages of the parameters of Boltzmann fits (as in Fig. 3B) for each individual experiment (see Table 1 for the numbers of experiments). *Error bars*, standard errors. *Lines* (*solid line*, brain channels; *dotted line*, muscle channels), least-squares fits to the data. A, Shift of the potential for half-maximal channel availability (V_h). Least-squares fits yield estimates of maximum voltage shifts of −40.6 ± 16.6 mV (mean ± standard error of the fit) for brain and −40.5 ± 13.8 mV for muscle channels, with EC_{50} values of 5.0 ± 3.8 mM and 5.0 ± 3.0 mM, respectively. B, Reduction of maximum current at hyperpolarized potentials (I_{max}), obtained from Boltzmann fits to channel availability plots (as shown in Fig. 3B). The least-squares fits yield IC_{50} values of 1.26 ± 0.07 and 1.13 ± 0.10 mM for brain and muscle channels, respectively.

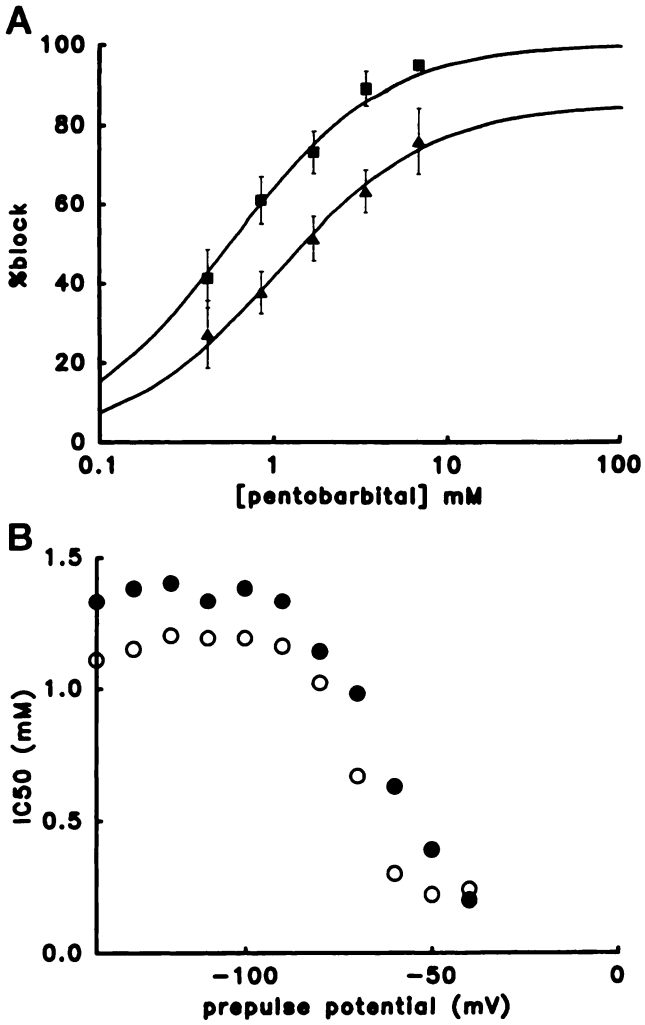

Fig. 5. Voltage dependence of pentobarbital inhibition. A, Comparison of pentobarbital inhibition for brain channel sodium currents elicited by voltage steps from −100 mV to −10 mV (▲) and from −60 mV to −10 mV (■). Inhibition was calulated as the reduction in channel availability at the specific potential, from data as shown in Fig. 3B. Averaged data from all experiments were used for the curve fits. *Error bars*, standard errors. Least-squares fits yield IC_{50} values for pentobarbital of 1.4 mM at −100 mV and 0.6 mM at −60 mV. B, Voltage dependence of the IC_{50} of pentobarbital. IC_{50} values were calculated from least-squares fits to curves as shown in A (●, brain channel; ○, muscle channel).

prolonged by pentobarbital in a concentration-dependent manner (Fig. 6B), consistent with fast association and dissociation rates for pentobarbital binding to the inactive state of the channel. If the prolonged recovery times were instead related to a slow rate of pentobarbital dissociation from the inactive state before the channel could reach the resting state, the population of channels with the slower recovery rates would increase but there would be no concentration-dependent increase in the time constant.

Use-dependent inhibition. A delay in the recovery of channel availability after a depolarization implies development of use-dependent inhibition. We therefore assessed use-dependent inhibition using trains of 20 pulses (28.5-msec long) to 0 mV from an interpulse potential of −85 mV. This use-dependent inhibition increases with frequency (Fig. 7A). Under control conditions, current declines very little even at 5-Hz stimulation frequency. Both the limiting sodium current in long trains of pulses and the time constant of current decay are decreased by pentobarbital, in a concentration-dependent manner (Fig. 7B).

Use-dependent inhibition could result from drug binding to open and/or to inactivated channels. To distinguish between these possibilities, we correlated use-dependent inhibition with the duration of the depolarizing pulses (Fig. 8A), the holding potential (Fig. 8B), and the test pulse potential (Fig. 8C). Increasing the depolarization duration from 4 msec to 20, 40, or 100 msec at constant interpulse intervals (500 msec, corresponding to a frequency of approximately 2 Hz) leads to a large increase in inhibition (Fig. 8A). Sodium channel activation is fast, and a depolarization of 4-msec

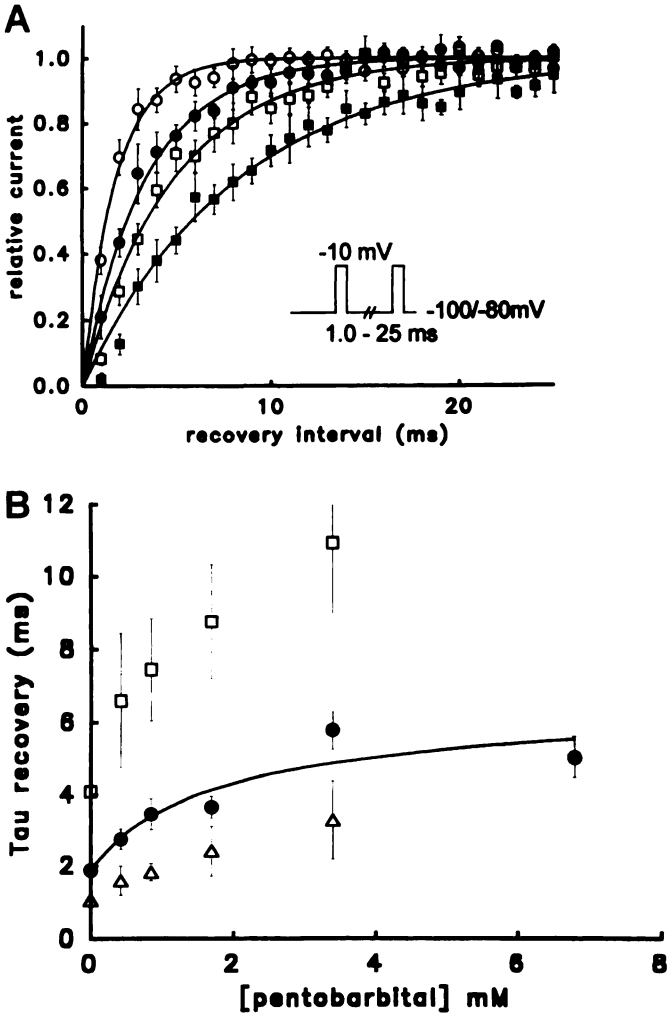

Fig. 6. Recovery of channel availability after depolarizing pulses. A, Recovery at different holding potentials. The pulse protocol included a reference pulse to −10 mV, a recovery interval of variable duration at −80, −100, or −120 mV, and a test pulse to −10 mV. Relative currents ($I/I_{reference}$) versus the length of the recovery interval for interpulse holding potentials of −100 mV (*circles*) and −80 mV (*squares*), before (*open symbols*) and after (*filled symbols*) superfusion with 0.85 mM pentobarbital, are shown. *Lines*, least-squares fits of a single-exponential function to the data, yielding time constants for recovery of 1.8 msec for controls at −100 mV, 3.4 msec with pentobarbital at −100 mV, 4.9 msec for controls at −80 mV, and 8.4 msec with pentobarbital at −80 mV. Data are from five cells expressing brain IIa sodium channels. B, Concentration dependence of the increase in the time constant of recovery (brain channels). Time constants (measured as described for A) at holding potentials of −100 mV (●), −120 mV (△), and −80 mV (□) are plotted versus pentobarbital concentration. *Line*, least-squares fit to the data at −100 mV, yielding an EC_{50} of 1.6 mM and a maximum time constant of 4.4 msec. Data are from 18 cells expressing brain sodium channels at −100 mV, seven cells at −120 mV, and 10 cells at −80 mV.

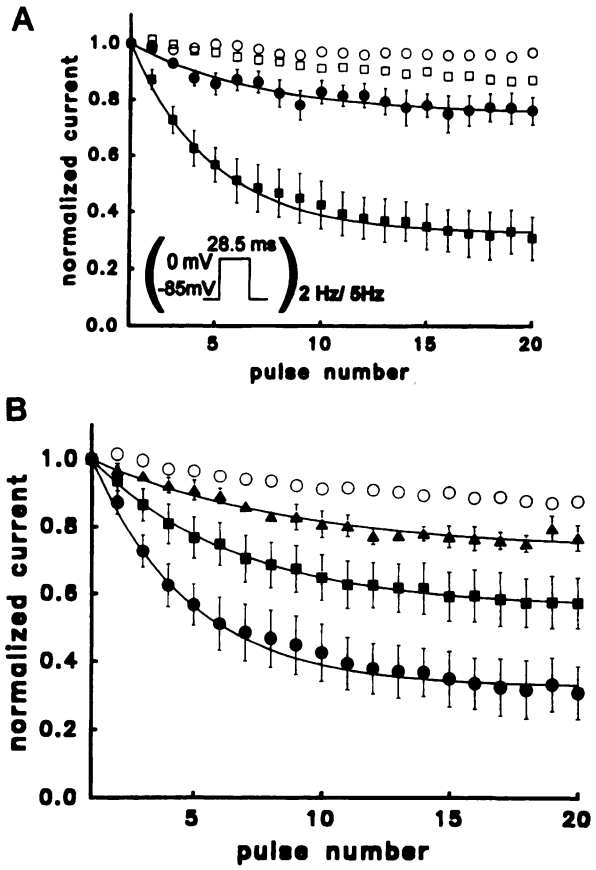

Fig. 7. Use-dependent inhibition. A, Frequency dependence of current reduction. Plotted are normalized currents elicited by trains of 20 pulses before (*open symbols*) and after (*filled symbols*) superfusion with 3.4 mM pentobarbital. Pulses to 0 mV (28.5 msec) from a holding potential of −85 mV were used. Currents are normalized to the first pulse. At 2 Hz (*circles*), 3.4 mM pentobarbital reduces the normalized limiting sodium current (obtained from least-squares fits to a single-exponential function) (*lines*) from 0.95 to 0.75, with a time constant of 3.0 msec. At 5 Hz (*squares*), 3.4 mM pentobarbital reduces the normalized limiting sodium current from 0.85 to 0.33, with a time constant of 0.76 msec. Data are averages from six cells expressing brain sodium channels. *Error bars*, standard error. B, Concentration dependence of use-dependent inhibition at 5 Hz. Shown are the currents obtained before (○) and after superfusion with 0.42 (▲), 1.7 (■), and 3.4 mM (●) pentobarbital (same cells as in A). Single-exponential fits (*lines*) yield normalized limiting sodium current values of 0.73, 0.56, and 0.33 at the indicated pentobarbital concentrations. The time constants of current decrease are 1.63, 1.13, and 0.76 msec, respectively.

duration is sufficient to open almost all available channels (see time course of sodium currents in Fig. 1); therefore, increasing the pulse duration results only in an increase in the time channels spend in the inactivated state.

Use-dependent inhibition is enhanced by more depolarized interpulse holding potentials (Fig. 8B), leading to a faster decay and a more pronounced reduction in the limiting sodium current. Hyperpolarized holding potentials remove use-dependent inhibition almost completely, although the number of channels opening is the same at all experimental potentials (except at −70 mV, where channel availability is already reduced; see channel availability curves in Fig. 3). Recovery of channel availability, on the other hand, is faster at more hyperpolarized potentials (Fig. 6) and can explain the removal of use-dependent inhibition. A larger use-dependent inhibition is also found with more positive test potentials (Fig. 8C). These findings can be consistently explained by a preferential binding of pentobarbital to the inactivated state of the sodium channel.

Discussion

Comparison of pentobarbital effects on brain IIa and muscle sodium channels. Rat brain IIa and rat muscle sodium channels have a sequence homology of 76.2% (22) and

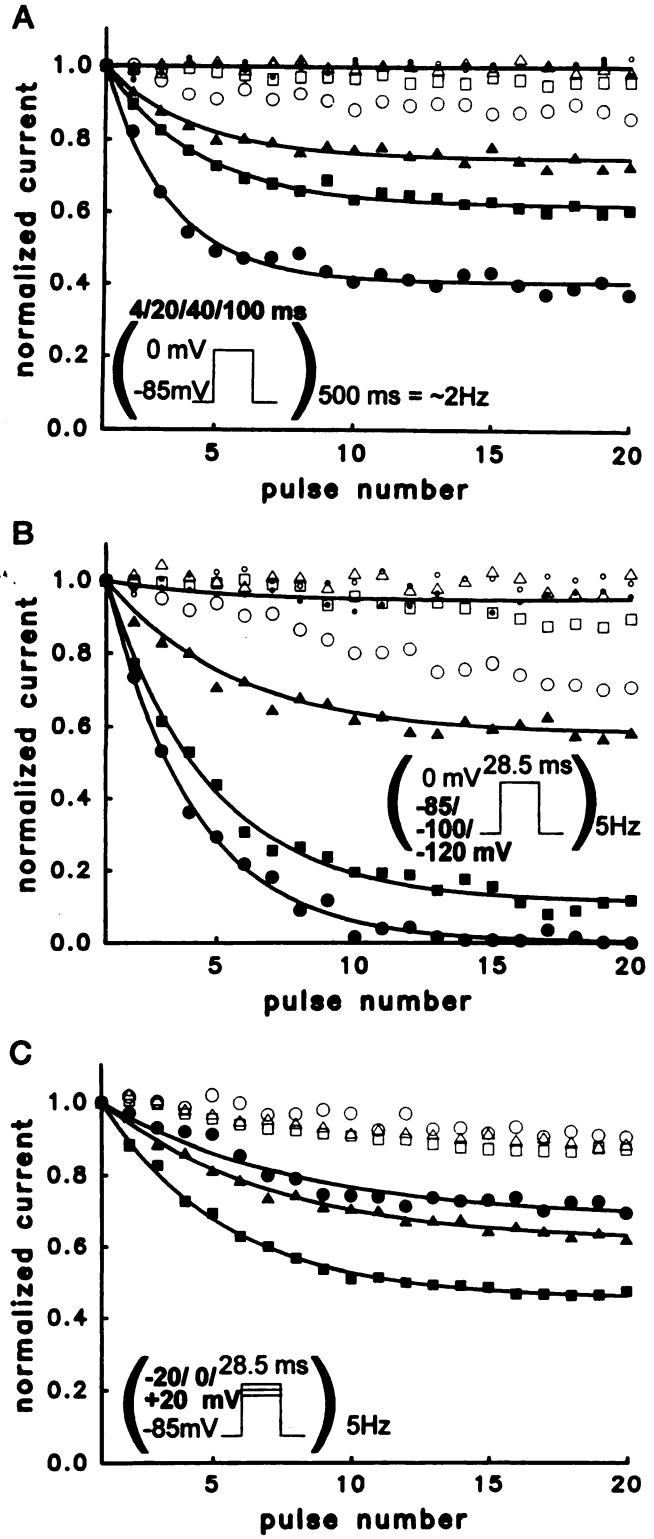

Fig. 8. Influence of potential and test pulse potential on use-dependent inhibition. A, Effect of depolarization (test pulse) duration. Test pulse durations were 4 msec (*small circles*), 20 msec (*triangles*), 40 msec (*squares*), and 100 msec (*large circles*); the recovery interval was kept constant at 500 msec, corresponding to a frequency of approximately 2 Hz. Test pulses were to 0 mV from a holding potential of −85 mV. Data are from a representative cell, before (*open symbols*) and after (*filled symbols*) superfusion with 3.4 mM pentobarbital. B, Effect of holding potential on use-dependent inhibition. Data are from a representative cell expressing brain sodium channels, stimulated at 5 Hz with 28.5-msec pulses to 0 mV from holding potentials of −120 mV (*small circles*), −100 mV (*triangles*), −85 mV (*squares*), and −70 mV (*large circles*), before (*open symbols*) and after (*filled symbols*) superfusion with 3.4 mM pentobarbital. C, Effect of test pulse potential. Data are from seven cells expressing brain sodium channels, stimulated at 5 Hz with 28.5-msec pulses from a holding potential of −85 mV to test potentials of −20 mV (*circles*), 0 mV (*triangles*), and +20 mV (*squares*), before (*open symbols*) and after (*filled symbols*) superfusion with 3.4 mM pentobarbital.

distinct pharmacological properties, such as different sensitivities to certain toxins (23). Despite these structural and pharmacological differences, however, concentration-response curves for pentobarbital suppression of these channels were found to be similar. This result parallels findings at the single-channel level in planar lipid bilayers (14). Furthermore, despite differences in the voltage dependence of channel inactivation of the two channels, the pentobarbital-induced shifts of the channel availability curves were identical.

These results suggest that the sites of pentobarbital interaction with the sodium channel are conserved regions of the channel protein. Alternatively, this could be explained by a pentobarbital-induced modulation of the physico-chemical properties of the lipid membrane, the molecular composition of which has been reported to influence pentobarbital suppression of sodium channel currents (24). The functional mechanisms by which pentobarbital reduced sodium channel currents were examined in the experiments presented here.

At most potentials, the IC_{50} of pentobarbital block is greater than the concentrations used clinically (50–200 μM, depending on criteria used for determination) (25, 26). At membrane potentials similar to that of resting neurons (−60 and −70 mV) (27), the IC_{50} values determined in our preparations are 200–600 μM for muscle sodium channels and 600–900 μM for brain channels (Fig. 5B). However, other factors also affect the sensitivity of the sodium channels, including frequencies of neuronal stimulation (Figs. 7 and 8), nerve fiber diameter, and ionic channel densities (28–30). Additionally, although the fraction of sodium channels blocked at these concentrations is <50%, it has been shown that changes in much smaller fractions of sodium channels can cause serious cellular dysfunction (31, 32). Finally, whereas only racemic mixtures of pentobarbital were used in the present studies, a previous examination of pentobarbital isomer interactions with the sodium channel found no differences in potency between the isomers. It has been reported that pentobarbital anesthesia is stereoselective, using sleep studies as a crude measure of anesthetic potency (33–35); however, the reported differences were a factor of 2 or less. Although the isomers of pentobarbital showed different potencies in some cellular interactions (36), the relevance of these interactions to pentobarbital anesthesia has not been resolved (37–40). Thus, although the role that sodium channels play in pentobarbital anesthesia is currently unclear, a significant fraction of these proteins would be blocked during clinical anesthesia.

Mechanisms of pentobarbital inhibition. Pentobarbital suppresses sodium currents by at least two distinct mechanisms, i.e., a direct suppression of resting (or open) channels, probably representing a potential-independent block, and an effect on the inactivation gating mechanism such that channels inactivate at more hyperpolarized potentials. Brain- and muscle-type sodium channels have similar differential sensitivities to these two mechanisms. Higher concen-

trations are needed to produce a half-maximal shift in channel availability than a half-maximal suppression of current at hyperpolarized potentials. Current suppression, measured as the reduction of the maximum current of standard current-voltage curves, parallels the dose dependence of inhibition at hyperpolarized potentials. Due to the complete recovery of channel availability before each depolarization (2 sec at −100 mV) when current-voltage curves are determined, the effect on channel availability is not perceptible. At more depolarized prepulse potentials, where channel availability is reduced, IC_{50} values are lower (Fig. 5B), due to the combined action of these effects of pentobarbital.

The pentobarbital-induced hyperpolarizing shift of steady state inactivation, determined from the fraction of channels not suppressed directly, can be explained using the modulated receptor model (4, 5). In this model drugs are assumed to bind to different channel states (at least three) with different affinities. The modulated receptor model can explain the shift in steady state channel availability, the slowed recovery of channel availability (Fig. 6), and the voltage dependence of the IC_{50} (Fig. 5B), if pentobarbital is assumed to bind with higher affinity to the inactivated state than to resting or open states.

The observed use-dependent inhibition, on the other hand, could also be due to binding to the open state of the channel. To examine this question, we used modifications of the protocol that increase the time sodium channels spend in the inactivated state. Increasing the length of depolarization or using more positive holding and test pulse potentials increased the extent of use-dependent inhibition. This indicates that use-dependent inhibition indeed results largely from pentobarbital binding to and stabilization of the inactivated state.

It should be kept in mind that currents are already reduced in the first pulse of the pulse trains used to measure use-dependent inhibition. A pentobarbital concentration reducing the current of the first pulse by 50% leads, at 5 Hz, to a further reduction of only about 40% of the already reduced amplitude. Thus, much of the total inhibition must result from binding to resting or open channels (tonic inhibition) or must be due to other mechanisms. However, higher stimulation frequencies and more depolarized prepulse potentials lead to increasing magnitudes of use-dependent inhibition.

The effect of pentobarbital on resting (or open) channels is represented by the current suppression after hyperpolarized prepulse potentials, as seen in Fig. 3B. Single-channel experiments may be necessary to gain additional insight into the mechanism of this part of pentobarbital inhibition. It is unclear whether the observed effects result from pentobarbital interaction with one binding site having variable affinity or interactions with multiple sites.

Comparison of pentobarbital with other sodium channel inhibitors. The effects of different classes of drugs, such as local anesthetics, antiarrhythmic agents, and anticonvulsants, on sodium channels have been described using the modulated receptor hypothesis (1). These drugs all cause a hyperpolarizing shift in the voltage dependence of channel availability and use-dependent inhibition.

Our results indicate that pentobarbital suppression of sodium channels also may be described with this hypothesis. Compared with lidocaine, which causes only very little current suppression at hyperpolarized prepulse potentials (3), pentobarbital has a higher affinity for resting or open channels. Similarly to lidocaine, however, pentobarbital has a relatively higher affinity for inactivated channels than resting and open channels (this is not the same for all local anesthetics; many local anesthetics have higher affinity for open channels) (41). The term "affinity," as used here, describes only the pharmacodynamic model, without implying specific binding to a receptor site.

Use-dependent inhibition of action potentials by pentobarbital has been shown to occur in myelinated nerve fibers, with the magnitude depending on the stimulation frequency (42) and also on the location of measurement along the axon (43). Activity-dependent processes such as facilitation (increased effectiveness of excitatory input produced by frequent stimulation) are probably important mechanisms of memory, and use-dependent inhibition is likely to inhibit the development of facilitation. Involvement of frequency-dependent effects (44) and disruption of the temporal integration of excitation and inhibition (45) have been proposed as mechanisms of anesthesia, but their significance remains to be proven.

The increasing potency of pentobarbital at depolarized potentials leads to a particularly high sodium current inhibition at threshold potentials for action potential firing. Volatile anesthetics have been shown to increase the firing threshold of axons (46), and pentobarbital may well have the same effect.

Acknowledgments

We wish to thank Dr. B. W. Urban for many helpful discussions and Dr. D. Gardner for comments on the manuscript. We are grateful to Dr. L. Palmer for allowing us to use his equipment.

References

1. Catterall, W. A. Common modes of drug action on Na-channels: local anesthetics, antiarrhythmics and anticonvulsants. *Trends Pharmacol. Sci.* **8**:57–65 (1987).
2. Hille, B. *Ionic Channels of Excitable Membranes*. Sinauer Associates, Sunderland, MA (1992).
3. Ragsdale, D. S., T. Scheuer, and W. A. Catterall. Frequency and voltage-dependent inhibition of type IIA Na^+ channels, expressed in a mammalian cell line, by local anesthetic, antiarrhythmic, and anticonvulsant drugs. *Mol. Pharmacol.* **40**:756–765 (1991).
4. Hille, B. Local anesthetics: hydrophilic and hydrophobic pathways for the drug-receptor reaction. *J. Gen. Physiol.* **69**:497–515 (1977).
5. Hondeghem, L. M., and B. G. Katzung. Time- and voltage-dependent interactions of anti-arrhythmic drugs with cardiac sodium channels. *Biochim. Biophys. Acta* **472**:373–398 (1977).
6. Trimmer, J. S., and W. S. Agnew. Molecular diversity of voltage-sensitive Na channels. *Annu. Rev. Physiol.* **51**:401–418 (1989).
7. Neumcke, B. Diversity of sodium channels in adult and cultured cells, in oocytes and in lipid bilayers. *Rev. Physiol. Biochem. Pharmacol.* **115**:1–49 (1990).
8. Narahashi, T., D. T. Frazier, T. Deguchi, C. A. Cleaves, and M. C. Ernau. The active form of pentobarbital in squid giant axons. *J. Pharmacol. Exp. Ther.* **177**:25–33 (1971).
9. Schwarz, J. R. The mode of action of phenobarbital on the excitable membrane of the node of Ranvier. *Eur. J. Pharmacol.* **56**:51–60 (1979).
10. Kendig, J. J., K. R. Courtney, and E. N. Cohen. Anesthetics: molecular correlates of voltage- and frequency-dependent sodium channel block in nerve. *J. Pharmacol. Exp. Ther.* **210**:446–452 (1979).
11. Urban, B. W., and D. A. Haydon. The actions of halogenated ethers on the ionic currents of the squid giant axon. *Proc. R. Soc. Lond. B Biol. Sci.* **231**:13–26 (1987).
12. Frenkel, C., D. S. Duch, and B. W. Urban. Molecular actions of pentobarbital isomers on sodium channels from human brain cortex. *Anesthesiology* **72**:640–649 (1990).
13. Frenkel, C., D. S. Duch, and B. W. Urban. Effects of i.v. anaesthetics on human brain sodium channels. *Br. J. Anaesth.* **71**:15–24 (1993).
14. Wartenberg, H. C., J. Wang, B. Rehberg, B. W. Urban, and D. S. Duch.

Molecular actions of pentobarbitone on sodium channels in lipid bilayers: role of channel structure. *Br. J. Anaesth.* **72**:668–673 (1994).
15. Scheuer, T., V. J. Auld, S. Boyd, J. Offord, R. Dunn, and W. A. Catterall. Functional properties of rat brain sodium channels expressed in a somatic cell line. *Science (Washington D. C.)* **247**:854–858 (1990).
16. West, J. W., T. Scheuer, L. Maechler, and W. A. Catterall. Efficient expression of rat brain type IIA Na^+ channel α subunits in a somatic cell line. *Neuron* **8**:59–70 (1992).
17. Urcan, M. S., S. S. Tinkle, E. Bennett, and S. R. Levinson. Stable expression of a rat muscle sodium channel in a CHO cell line. *Mol. Biol. Cell* **3**:301a (1992).
18. Bennett, E., V. V. Patel, S. S. Tinkle, M. S. Urcan, and S. R. Levinson. Effect of *N*-glycosylation on sodium channel gating. *Biophys. J.* **66**:A102 (1994).
19. Hamill, O. P., A. Marty, E. Neher, B. Sakmann, and F. J. Sigworth. Improved patch-clamp techniques for high-resolution current recording from cells and cell-free membrane patches. *Pflügers Arch.* **391**:85–100 (1981).
20. Fernandez, J. M., A. P. Fox, and S. Krasne. Membrane patches and whole-cell membranes: a comparison of electrical properties in rat clonal pituitary (GH_3) cells. *J. Physiol. (Lond.)* **356**:565–585 (1984).
21. Elliott, A. A., and J. R. Elliott. The role of inactivation in the effects of *n*-alkanols on the sodium current of cultured sensory neurons. *J. Physiol. (Lond.)* **415**:19–33 (1989).
22. Trimmer, J. S., S. S. Cooperman, S. A. Tomiko, J. Zhou, S. M. Crean, M. B. Boyle, R. G. Kallen, Z. Sheng, R. L. Barchi, F. J. Sigworth, R. H. Goodman, W. S. Agnew, and G. Mandel. Primary structure and functional expression of a mammalian skeletal muscle sodium channel. *Neuron* **3**:33–49 (1989).
23. Moczydlowski, E., B. Olivera, W. R. Gray, and G. Strichartz. Discrimination of muscle and neuronal Na channel subtypes by binding competition between [^{3}H]saxitoxin and μ-conotoxin. *Proc. Natl. Acad. Sci. USA* **83**: 5321–5325 (1986).
24. Rehberg, B., B. W. Urban, and D. S. Duch. The membrane lipid cholesterol modulates anesthetic actions on a human brain ion channel. *Anesthesiology* **82**:749–758 (1995).
25. Bolander, H. G., G. Wahlstrom, and L. Norberg. Reevaluation of potency and pharmacokinetic properties of some lipid-soluble barbiturates with an EEG-threshold method. *Acta Pharmacol. Toxicol.* **54**:33–40 (1984).
26. Bayliff, C. D., M. L. Schwartz, and B. G. Hardy. Pharmacokinetics of high-dose pentobarbital in severe head trauma. *Clin. Pharmacol. Ther.* **38**:457–461 (1985).
27. Kandel, E. R., J. H. Schwartz, and T. M. Jessel. *Principles of Neural Science*, Ed. 3. Elsevier Science Publishing Co., New York, 160 (1991).
28. Raymond, S. A. Sub-blocking concentrations of local anesthetics: effects on impulse generation and conduction in single myelinated sciatic nerve axons in frog. *Anesth. Analg.* **75**:906–921 (1992).
29. Butterworth, J. F., S. A. Raymond, and R. F. Roscoe. Effects of halothane and enflurane on firing threshold of frog myelinated axons. *J. Physiol. (Lond.)* **411**:493–516 (1989).
30. Mandel, G. Tissue specific expression of the voltage-sensitive sodium channel. *J. Membr. Biol.* **125**:193–205 (1992).
31. Cannon, S. C., R. H. Brown, and D. P. Corey. Theoretical reconstruction of myotonia and paralysis caused by incomplete inactivation of sodium channels. *Biophys. J.* **65**:270–288 (1993).
32. Narahashi, T. Nerve membrane Na channels as targets of insecticides. *Trends Pharmacol. Sci.* **13**:236–241 (1992).
33. Christensen, H. D., and I. S. Lee. Anesthetic potency and acute toxicity of optically active disubstituted barbituric acids. *Toxicol. Appl. Pharmacol.* **26**:495–503 (1973).
34. Freudenthal, R. I., and J. Martin. Correlation of brain levels of barbiturate enantiomers with reported differences in duration of sleep. *J. Pharmacol. Exp. Ther.* **193**:664–668 (1975).
35. Cook, C. E., T. B. Seltzman, C. R. Tallent, B. Lorenzo, and D. E. Drayer. Pharmacokinetics of pentobarbital enantiomers as determined by enantioselective radioimmunoassay after administration of racemate to humans and rabbits. *J. Pharmacol. Exp. Ther.* **241**:779–785 (1987).
36. Roth, S. H., and K. W. Miller, eds. *Molecular and Cellular Mechanisms of Anesthetics*. Plenum Publishing Co., New York (1986).
37. Andrews, P. R., and L. C. Mark. Structural specificity of barbiturates and related drugs. *Anesthesiology* **57**:314–320 (1982).
38. Owen, D. G., J. L. Barker, M. Segal, and R. E. Study. Postsynaptic actions of pentobarbital in cultured mouse spinal neurons and rat hippocampal neurons, in *Molecular and Cellular Mechanisms of Anesthetics* (S. H. Roth and K. W. Miller, eds.). Plenum Publishing Co., New York, 27–41 (1986).
39. Olsen, R. W. Barbiturates. *Int. Anesthesiol. Clin.* **26**:254–261 (1988).
40. Dolin, S. J., M. J. Halsey, and H. J. Little. Effects of the calcium channel activator Bay K 8644 on general anesthetic potency in mice. *Br. J. Pharmacol.* **94**:413–422 (1988).
41. Butterworth, J. F., and G. R. Strichartz. Molecular mechanisms of local anesthesia: a review. *Anesthesiology* **72**:711–734 (1990).
42. Strichartz, G. Use-dependent conduction block produced by volatile general anesthetic agents. *Acta Anaesth. Scand.* **24**:402–406 (1980).
43. Grossman, Y., and J. J. Kendig. General anesthetic block of a bifurcating axon. *Brain Res.* **245**:148–153 (1982).
44. Kendig, J. J. Neuronal basis of the anesthetic state, in *General Anaesthesia* (J. F. Nunn, J. E. Utting, and B. R. Brown, eds.). Butterworths, London, 30–37 (1989).
45. Urban, B. W. Differential effects of gaseous and volatile anaesthetics on sodium and potassium channels. *Br. J. Anaesth.* **71**:25–38 (1993).
46. Butterworth, J. F., S. A. Raymond, and R. F. Roscoe. Effects of halothane and enflurane on firing threshold of frog myelinated axons. *J. Physiol. (Lond.)* **411**:493–516 (1989).

Send reprint requests to: Daniel N. S. Duch, Department of Anesthesiology, Room A-1030, Cornell University Medical College, 1300 York Ave., New York, NY 10021.